Visual pigment–deficient cones survive and mediate visual signaling despite the lack of outer segments

Hui Xu[a,b,1], Nange Jin[c,1,2], Jen-Zen Chuang[d,1], Zhao Zhang[b], Xiaoyue Zhong[b], Zhijing Zhang[c,2], Ching-Hwa Sung[d,e,3], Christophe P. Ribelayga[c,2,3], and Yingbin Fu[a,b,3]

[a]Interdepartmental Program in Neuroscience, University of Utah, Salt Lake City, UT 84132; [b]Department of Ophthalmology, Baylor College of Medicine, Houston, TX 77030; [c]Ruiz Department of Ophthalmology and Visual Science, The University of Texas Health Science Center at Houston, Houston, TX 77030; [d]Department of Ophthalmology, Weill Cornell Medicine, New York, NY 10065; and [e]Department of Cell and Developmental Biology, Weill Cornell Medicine, New York, NY 10065

Edited by King-Wai Yau, The Solomon H. Snyder Department of Neuroscience, Johns Hopkins University School of Medicine, Baltimore, MD; received August 16, 2021; accepted December 30, 2021

Rhodopsin and cone opsins are essential for light detection in vertebrate rods and cones, respectively. It is well established that rhodopsin is required for rod phototransduction, outer segment disk morphogenesis, and rod viability. However, the roles of cone opsins are less well understood. In this study, we adopted a loss-of-function approach to investigate the physiological roles of cone opsins in mice. We showed that cones lacking cone opsins do not form normal outer segments due to the lack of disk morphogenesis. Surprisingly, cone opsin–deficient cones survive for at least 12 mo, which is in stark contrast to the rapid rod degeneration observed in rhodopsin-deficient mice, suggesting that cone opsins are dispensable for cone viability. Although the mutant cones do not respond to light directly, they maintain a normal dark current and continue to mediate visual signaling by relaying the rod signal through rod–cone gap junctions. Our work reveals a striking difference between the role of rhodopsin and cone opsins in photoreceptor viability.

cone opsin | rod–cone gap junction | cone photoreceptor | rod photoreceptor

Two types of photoreceptors are involved in image-forming vision in the vertebrate retina: rods and cones. Rods are responsible for dim light vision, whereas cones mediate bright light and color vision. Both rods and cones rely on visual pigments that are embedded in their outer segment discs for light detection. Rods express one type of visual pigment, rhodopsin, whereas cones express different types of cone opsins for detecting light with different wavelengths (1, 2). The fundamental function of rhodopsin and cone opsins in phototransduction has been well established (3, 4). In addition to phototransduction, rhodopsin also has a structural role in disk membrane formation (5–7). In particular, rhodopsin-null mice ($Rho^{-/-}$) did not form outer segments and underwent rod degeneration within ∼90 d, suggesting rhodopsin is important for rod cell survival (6, 7).

In contrast to the wealth of information available on rhodopsin, much less is known about cone opsins despite their important role in mediating daylight vision and high-acuity vision. To better understand the function of cone opsins, we took a loss-of-function approach to study the role of cone opsins on the structure and function of cone photoreceptors. Because some mouse cones coexpress the medium-wavelength sensitive opsin (M-opsin encoded by *Opn1mw*) and short-wavelength sensitive opsin (S-opsin encoded by *Opn1sw*), we first generated the $Opn1mw^{-/-}$ mice and subsequently crossed them with the $Opn1sw^{-/-}$ mice (8) to generate the $Opn1sw^{-/-}Opn1mw^{-/-}$ mice. In this study, we performed morphological, ultrastructural, and physiological studies on $Opn1sw^{-/-}$ $Opn1mw^{-/-}$ cones in comparison to wild-type (WT) cones. We show that in contrast to rhodopsin, cone opsins are dispensable for cone viability despite their essential role in outer segment disk morphogenesis. $Opn1sw^{-/-}Opn1mw^{-/-}$ cones do not respond to light; however, they maintain a normal dark current and continue to mediate visual signaling by relaying the rod signal through rod–cone gap junctions.

Results

Long-Term Survival of Cone Photoreceptors without Cone Opsins. We bred $Opn1mw^{-/-}$ (9) with $Opn1sw^{-/-}$ (8) mice to generate the $Opn1sw^{-/-}Opn1mw^{-/-}$ mice. We confirmed the absence of both M-opsin and S-opsin in the $Opn1sw^{-/-}Opn1mw^{-/-}$ retina, while rhodopsin was located normally in the rod outer segment (ROS) (Fig. 1*A*). $Opn1sw^{-/-}Opn1mw^{-/-}$ cones showed normal morphology except with much shorter length of inner plus outer segment as determined by labeling with the cone cell marker, cone arrestin (Fig. 1*B*). Quantitative assessment showed that the overall length of inner plus outer segment was reduced by 41, 56, and 54% in 1-, 6-, and 12-mo-old $Opn1sw^{-/-}$ $Opn1mw^{-/-}$ mice, respectively, in comparison with WT (Fig. 1*C*). This was primarily due to the lack of an outer segment of $Opn1sw^{-/-}Opn1mw^{-/-}$ cones because the inner segment length of $Opn1sw^{-/-}Opn1mw^{-/-}$ cones was only slightly reduced

Significance

The study of visual pigments (rhodopsin in rods and cone opsins in cones) in vision has a long and illustrious history. It is well established that rhodopsin is required for rod phototransduction, outer segment formation, and rod viability. It is not known if the same is true for the cones. By using the cone opsin–deficient mice, we made the surprising observation that cones survive for at least 12 mo without cone opsins, suggesting that cone opsins are dispensable for cone viability. Furthermore, cone opsin–deficient cones continue to mediate visual signaling by relaying the rod signal through rod–cone gap junctions. Our finding represents a major difference between the two types of photoreceptors in vertebrates: rods and cones.

Author contributions: C.-H.S., C.P.R., and Y.F. designed research; H.X., N.J., J.-Z.C., Zhao Zhang, X.Z., Zhijing Zhang, and C.P.R. performed research; H.X., N.J., J.-Z.C., Zhao Zhang, C.-H.S., C.P.R., and Y.F. analyzed data; and C.-H.S., C.P.R., and Y.F. wrote the paper.

The authors declare no competing interest.

This article is a PNAS Direct Submission.

[1]H.X., N.J., and J.-Z.C. contributed equally to this work.

[2]Present address: Department of Vision Sciences, The University of Houston College of Optometry, Houston, TX 77204.

[3]To whom correspondence may be addressed. Email: chsung@med.cornell.edu, cpribela@central.uh.edu, or yingbin.fu@bcm.edu.

This article contains supporting information online at http://www.pnas.org/lookup/suppl/doi:10.1073/pnas.2115138119/-/DCSupplemental.

Published February 23, 2022.

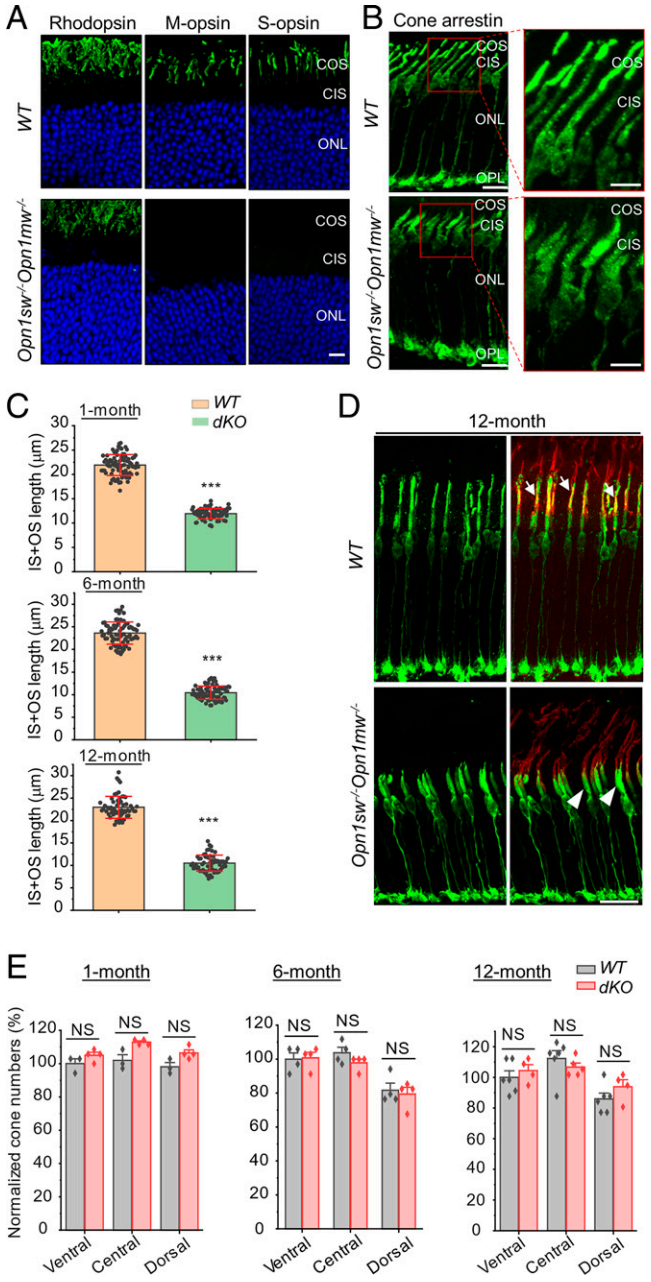

Fig. 1. Long-term survival of *Opn1sw*$^{-/-}$*Opn1mw*$^{-/-}$ cones. (*A*) Retinal sections from 1-mo-old WT and *Opn1sw*$^{-/-}$*Opn1mw*$^{-/-}$ mice were immunostained with antibodies against rhodopsin, M-opsin, and S-opsin. (*B*) Cones of 1-mo-old WT and *Opn1sw*$^{-/-}$*Opn1mw*$^{-/-}$ mice were visualized by labeling cone arrestin in retinal sections. (*Right*) Magnified views of two boxed regions from *Left*. (*C*) Quantitative comparison of IS plus OS length between WT and *Opn1sw*$^{-/-}$*Opn1mw*$^{-/-}$ (*dKO*) mice. Data represent mean ± SD. ***$P < 0.001$. $N = 80$ cones from 1- and 6-mo-old mice for both genotypes (4 WT, 4 *dKO*, 20 cones per mouse), $n = 60$ cones from 12-mo-old mice for both genotypes (3 WT, 3 *dKO*, 20 cones per mouse). Statistics were performed with unpaired two-sample *t* test. (*D*) Retinal sections from 12-mo-old WT and *Opn1sw*$^{-/-}$*Opn1mw*$^{-/-}$ mice were labeled with anti-mouse cone arrestin antibody (in green) and rhodamine PNA (in red). Arrows indicate colocalization between cone arrestin and PNA in the outer segment of WT, while white arrowheads indicate cone arrestin in the inner segment of *Opn1sw*$^{-/-}$*Opn1mw*$^{-/-}$ mice. (*E*) Quantitative results of relative cone numbers at the ventral, central, and dorsal retina from 1-, 6-, and 12-mo-old WT and *Opn1sw*$^{-/-}$*Opn1mw*$^{-/-}$ mice. Data (mean ± SEM) were normalized to WT ventral region. $N = 3$ to 4 (1 mo), 4 (6 mo), and 4 to 6 (12 mo) for each genotype. The difference between WT and *Opn1sw*$^{-/-}$*Opn1mw*$^{-/-}$ mice was not significant (NS) for all comparisons by one-way ANOVA with Tukey post hoc analysis. IS, inner segment. (Scale bar, 10 μm in *A* and *B*, *Left*; 5 μm in *B*, *Right*; and 20 μm in *D*.)

compared with WT cones (*SI Appendix*, Fig. S1). In other words, the mean length differences of 10.0, 13.2, and 12.4 μm largely reflected the length of WT cone outer segment (COS) at 1-, 6-, and 12-mo, respectively. WT cone arrestin showed strong expression in the COS and synaptic terminal (Fig. 1*D* and *SI Appendix*, Fig. S2, arrows indicating strong colocalization signal between cone arrestin in green and peanut agglutinin [PNA] in red in the outer segment in WT). This pattern was shifted to the cone inner segment (CIS) and synaptic terminal due to the lack of normal COS in *Opn1sw*$^{-/-}$*Opn1mw*$^{-/-}$ mice (Fig. 1*D* and *SI Appendix*, Fig. S2, white arrowheads indicating localization of cone arrestin in the inner segment). Labeling of PNA (in red) showed long cone matrix sheaths in *Opn1sw*$^{-/-}$*Opn1mw*$^{-/-}$ mice that were comparable to WT. Cone cell densities were similar between *Opn1sw*$^{-/-}$*Opn1mw*$^{-/-}$ and WT mice in all regions at 1 mo of age (Fig. 1 *E*, *Left*). Moreover, *Opn1sw*$^{-/-}$*Opn1mw*$^{-/-}$ cones survived an extended time. There was no significant difference in cone density between *Opn1sw*$^{-/-}$*Opn1mw*$^{-/-}$ and WT mice in all retinal regions at 6 and 12 mo of age, suggesting that cone viability is unaffected in the absence of cone opsins at least until 1 y of age (Fig. 1 *D* and *E* and *SI Appendix*, Fig. S2). These observations are in sharp contrast to the rapid rod degeneration observed in *Rho*$^{-/-}$ mice (6, 7).

Ultrastructure of COS in *Opn1sw*$^{-/-}$*Opn1mw*$^{-/-}$ mice. To further examine the morphology of *Opn1sw*$^{-/-}$*Opn1mw*$^{-/-}$ cones, especially the COS in high resolution, we performed electron microscopy using biotinylated PNA to unequivocally identify cones in the rod-dominant retina of 6-wk-old WT and *Opn1sw*$^{-/-}$*Opn1mw*$^{-/-}$ mice (Fig. 2 *A* and *B*; arrows show silver-gold particles surrounding cones). The specificity of this technique in labeling cones was demonstrated in *SI Appendix*, Fig. S3 (no silver-gold particles in either the ROS in *SI Appendix*, Fig. S3*A*, or rod inner segment [RIS] in *SI Appendix*, Fig. S3*B*). As expected, the COS of WT contained stacked discs (Fig. 2*A*). In sharp contrast, the PNA-identified cones did not form typical COS in *Opn1sw*$^{-/-}$ *Opn1mw*$^{-/-}$ mice (Fig. 2*B*). The residual COS contained disorganized internal membranes. These observations are consistent with COS formation being initiated by the growth of opsin-containing membrane with retinal degeneration slow (RDS/peripherin-2)-mediated rim formation as a secondary step (10).

Trafficking of Cone Phototransduction Proteins. To determine whether the absence of opsins and normal disk membranes in the *Opn1sw*$^{-/-}$ *Opn1mw*$^{-/-}$ cones affect the trafficking of cone phototransduction proteins, we examined the subcellular localization of guanylate cyclase 1 (GC1), G protein coupled receptor kinase 1 (GRK1), cone transducin alpha subunit ($G_{\alpha}t2$), and cone cyclic nucleotide-gated (CNG) channel A3 subunit in WT and *Opn1sw*$^{-/-}$ *Opn1mw*$^{-/-}$ cones. In WT retinas, GC1 and GRK1 were expressed in both ROS and COS with a higher expression in cones (Fig. 3 *A* and *B*, Left, arrows; cones were colabeled with rhodamine-PNA in red). In *Opn1sw*$^{-/-}$ *Opn1mw*$^{-/-}$ retina, both GC1 and GRK1 were markedly reduced in cones, although their expression in rods was normal (Fig. 3 *A* and *B*, *Right*). In fact, we were not able to reliably detect either GC1 or GRK1 expression above the background signal. Similarly, $G_{\alpha}t2$ was absent in *Opn1sw*$^{-/-}$*Opn1mw*$^{-/-}$ cones (Fig. 3 *C*, *Right*) in contrast to the robust signal in WT cones (Fig. 3 *C*, *Left*, white arrows). Cone CNGA3 subunit was markedly reduced (Fig. 3*D*, white arrowheads) compared with that in WT cones (Fig. 3*D*, white arrows). Thus, cone opsins

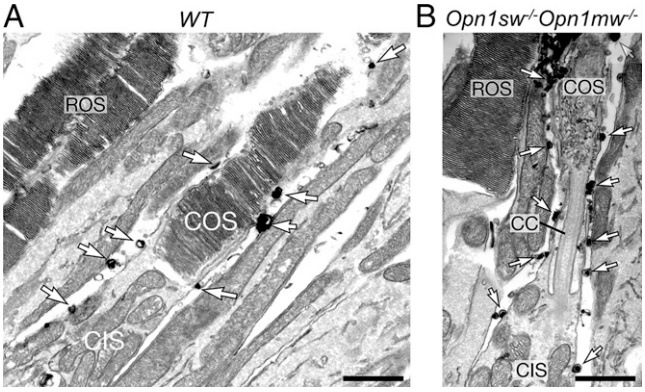

Fig. 2. Ultrastructure of WT and *Opn1sw*$^{-/-}$*Opn1mw*$^{-/-}$ cones. Cones in (*A*) WT and (*B*) *Opn1sw*$^{-/-}$*Opn1mw*$^{-/-}$ mice labeled with biotinylated PNA were visualized by silver enhanced streptavidin-conjugated gold particles. Electron-dense silver-gold particles surrounding COS and CIS were readily observed (arrows). ROS and RIS are not labeled. Also see *SI Appendix*, Fig. S3. CC, connecting cilium; RIS, rod inner segment. (Scale bar, 1 μm in *A* and *B*.)

and normal disk formation are required for the stability and trafficking of cone phototransduction proteins.

In addition to cone phototransduction proteins, we also examined the localization of two structural proteins, peripherin-2 (Prph2) and prominin-1 (Prom1). Both Prph2 and Prom1 are important for disk morphogenesis in rods and cones (11–17). As expected, Prom1 was normally restricted at the base of both ROS and COS in WT mice (Fig. 3 *E* and *G*, white arrows indicating Prom1 in cones). In *Opn1sw*$^{-/-}$*Opn1mw*$^{-/-}$ cones, Prom1 was mislocalized to the inner segment (Fig. 3*E*, white arrowheads, and Fig. 3*G*, white brackets) or localized at the base of COS (Fig. 3 *E* and *G*, yellow arrows). Prph2 was normally expressed throughout the outer segments of both rods and cones (Fig. 3 *F* and *H*, white arrows indicating signal in cones). In *Opn1sw*$^{-/-}$*Opn1mw*$^{-/-}$ mice, while Prph2 expression remained in the ROS, it appeared as dots at the base of residual COSs (Fig. 3 *F* and *H*, white arrowheads). In this experiment, we used cone arrestin and PNA double labeling (Fig. 3*I*) as a reference to help identify the junction of COS and CIS in the PNA/Prom1 and PNA/Prph2 labeled cones in Fig. 3 *G* and *H* (cone arrestin showed stronger signal in COS than in CIS, with red arrows indicating the junction of COS and CIS; see legend for details).

Functional Evaluation of Cone Photoreceptors by Electroretinography. To evaluate the photoreceptor function of *Opn1sw*$^{-/-}$ *Opn1mw*$^{-/-}$ and three control mouse lines (*Opn1sw*$^{-/-}$, *Opn1mw*$^{-/-}$, and WT), we performed photopic and scotopic electroretinography (ERG) recordings. Photopic ERG responses were not detectable in *Opn1sw*$^{-/-}$*Opn1mw*$^{-/-}$ mice to either 504-nm (λ_{max} for M-opsin) or 360-nm (λ_{max} for S-opsin) light stimuli, confirming the essential role of M-opsin and S-opsin for green and UV light detection, respectively (Fig. 4 *A* and *B*). As some mouse cone photoreceptors coexpress both S- and M-opsins, loss of either one would lead to the increase of the other through transcriptional compensation (8, 18). Indeed, the photopic ERG responses of *Opn1mw*$^{-/-}$ mice at 360 nm were enhanced at high intensities (Fig. 4*B*), which was likely due to the increased S-opsin level (9). Similarly, the photopic ERG responses of *Opn1sw*$^{-/-}$ mice to green light (504 nm) were slightly increased (Fig. 4*A*), which was consistent with increased M-opsin level (8).

Scotopic ERG reflects rod input at low intensities and mixed rod and cone input at high intensities. Both the scotopic a-wave and b-wave amplitudes were reduced in *Opn1sw*$^{-/-}$ *Opn1mw*$^{-/-}$ mice compared with the other three genotypes (Fig. 4 *C* and *D*). Because the cone sheaths are disordered (*SI Appendix*, Fig. S3*B*, arrows) and the normal traction system for transporting shed cone discs across the gap between the COS tip and the retinal pigment epithelium is likely compromised in *Opn1sw*$^{-/-}$ *Opn1mw*$^{-/-}$ mice, this might lead to an accumulation of extracellular debris in the subretinal space that is deleterious to rods. Indeed, we found that the length of outer nuclear layer (ONL) was reduced by 3.3, 4.7, and 8.2% in 1-, 6-, and 12-mo-old *Opn1sw*$^{-/-}$*Opn1mw*$^{-/-}$ mice, respectively, compared with those in age-matched WT (*SI Appendix*, Fig. S4), although no significant changes were observed for the length of ROS at 1 mo of age when ERG was recorded (*SI Appendix*, Fig. S5; see more in *Discussion*).

***Opn1sw*$^{-/-}$*Opn1mw*$^{-/-}$ Cones Mediate Rod Signaling via Rod–Cone Coupling.** In addition to mediating COS-originated intrinsic cone photoresponses, WT cones receive extrinsic rod inputs through rod–cone coupling, which are mediated by gap junctions (19–22). We performed electrophysiological recordings to investigate whether *Opn1sw*$^{-/-}$*Opn1mw*$^{-/-}$ cones receive rod-originated signals via rod–cone coupling despite the lack of intrinsic photoresponses. The cone photovoltages to 500- or 350-nm light were recorded at cone pedicles from retinal slices of different mouse lines to selectively stimulate the M-opsin or S-opsin, respectively (Fig. 5, green traces for 500 nm and blue traces for 350 nm). At 500 nm, WT cones exhibited an initial transient and fast component reflecting the contribution of the cone intrinsic response and a slower and long-lasting component reflecting the contribution of coupled rods (Fig. 5, *Top Left*, and *SI Appendix*, Fig. S6 *A* and *E*). In contrast, the fast component was absent in *Opn1sw*$^{-/-}$*Opn1mw*$^{-/-}$ cones, and they only showed the slow rod-mediated response (Fig. 5, *Bottom Left*, and *SI Appendix*, Fig. S6 *D* and *H*). The threshold intensity T_{500} (the light intensity required to elicit 0.5 mV response to 500 nm light), which was mainly driven by the rod input, was similar in *Opn1sw*$^{-/-}$*Opn1mw*$^{-/-}$ and WT cones (0.74 photons/μm^2/20-ms versus 0.64 photons/μm^2/20-ms; Table 1). Although the threshold intensity T_{350} to 350 nm light was approximately two times higher in *Opn1sw*$^{-/-}$*Opn1mw*$^{-/-}$ cones than in WT cones, this difference was not statistically significant ($P > 0.05$ between four genotypes in Table 1 among all cone recordings with rod input by two-way ANOVA). Application of the rod–cone gap junction blocker meclofenamic acid (MFA) (23, 24) eliminated the slow rod component in WT cones while abolishing all light responses in *Opn1sw*$^{-/-}$ *Opn1mw*$^{-/-}$ cones. This indicates that *Opn1sw*$^{-/-}$*Opn1mw*$^{-/-}$ cones mediate rod signaling via rod–cone coupling (Fig. 5, *Top Right* and *Bottom Right*, and *SI Appendix*, Fig. S6 *D* and *H*). As a control, deletion of S-opsin in *Opn1sw*$^{-/-}$ or M-opsin in *Opn1mw*$^{-/-}$ cones eliminated the fast cone response to UV or green light, respectively, while the remaining slow rod response persisted. This rod-mediated component was eliminated upon gap junction blocking (Fig. 5, *Middle*; *SI Appendix*, Fig. S6 *B*, *C*, *F*, and *G*; and Table 1). Finally, the rod photoresponses (recorded from the rod somata) to 500-nm light were not significantly different across all four genotypes (Table 1).

Since rod–cone coupling was mediated by connexin36 (Cx36), we compared the expression and distribution of Cx36 between WT and *Opn1sw*$^{-/-}$*Opn1mw*$^{-/-}$ retinas. Similar to the distribution of Cx36 in the WT retina (Fig. 6 *A*–*C*) (21), Cx36 was expressed in the outer plexiform layer (OPL) and inner plexiform layer (IPL) on *Opn1sw*$^{-/-}$*Opn1mw*$^{-/-}$ retinal sections (Fig. 6*D*), associated with cone telodendria (Fig. 6*E*), and at contact sites between rod spherules and cone telodendria (Fig. 6*F*, white arrows). Quantitative analysis showed that the number of Cx36 puncta/cone pedicle and the median volume of Cx36 puncta were similar between both genotypes (Fig. 6*G*), suggesting intact rod–cone coupling in *Opn1sw*$^{-/-}$*Opn1mw*$^{-/-}$

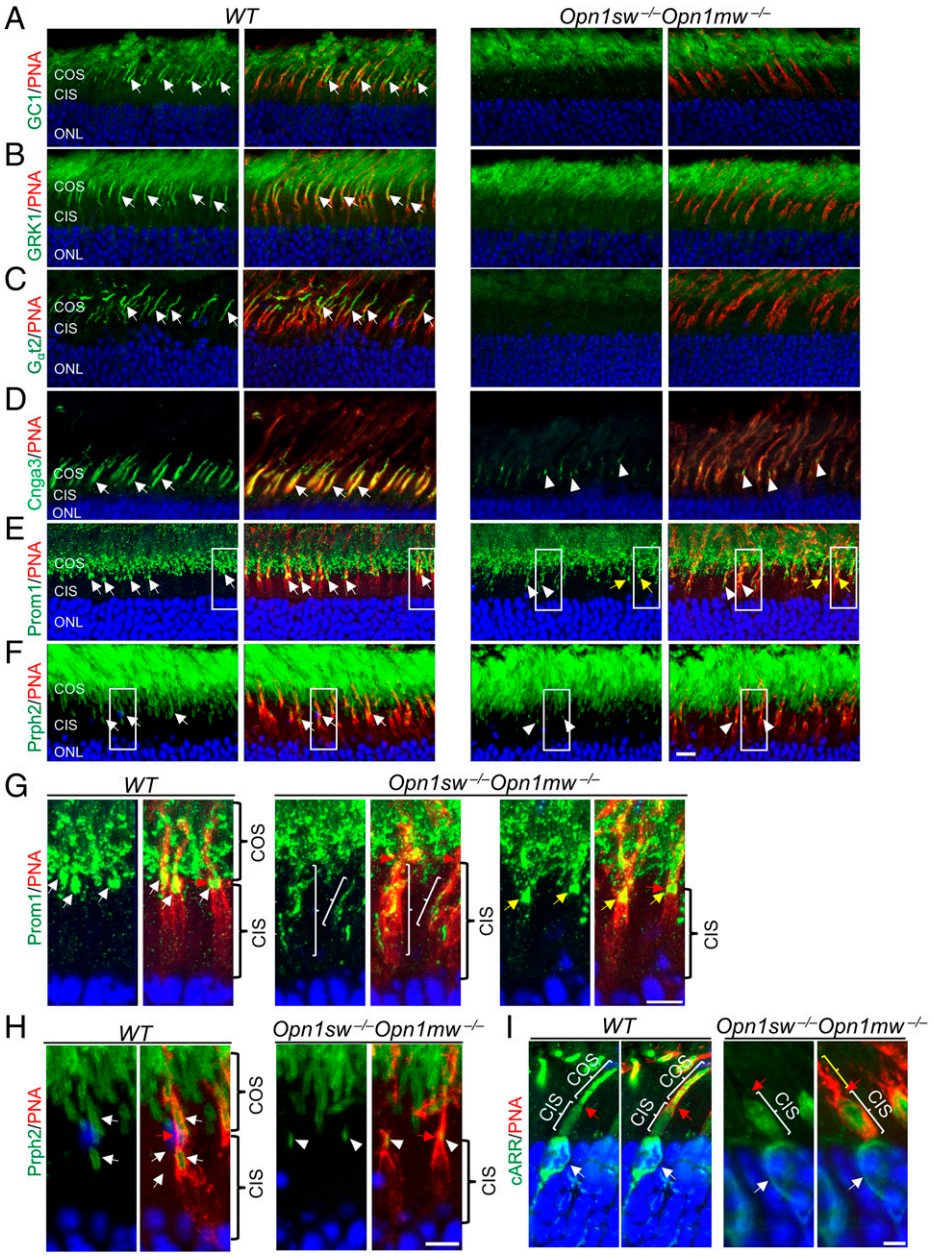

Fig. 3. Localization of outer segment membrane proteins in WT and *Opn1sw*$^{-/-}$*Opn1mw*$^{-/-}$ cones. Retinal sections from 1-mo-old WT and *Opn1sw*$^{-/-}$ *Opn1mw*$^{-/-}$ mice were stained with antibodies against (*A*) GC1, (*B*) GRK1, (*C*) G_{α}t2, (*D*) CNGA3, (*E*) Prom1, and (*F*) Prph2. White arrows and white arrowheads indicate the signal of various proteins in WT and *Opn1sw*$^{-/-}$*Opn1mw*$^{-/-}$ cones (in green), respectively. For Prom1, white arrowheads indicate its localization in CIS, while yellow arrows indicate its localization at the base of COS of *Opn1sw*$^{-/-}$*Opn1mw*$^{-/-}$ mice. (*G* and *H*) Magnified views of boxed regions in *E* and *F*, respectively. White arrows and white arrowheads indicate the signal of Prom1 or Prph2 in WT and *Opn1sw*$^{-/-}$*Opn1mw*$^{-/-}$ cones, respectively. White brackets indicate mislocalization of Prom1 in the inner segment. (*I*) Cone arrestin (cARR) and PNA double labeling to help identify COS and CIS in PNA/Prom1 and PNA/Prph2 labeled cones in *G* and *H*. In WT, cARR showed stronger labeling of the COS than the CIS. In *Opn1sw*$^{-/-}$*Opn1mw*$^{-/-}$ retina, cARR antibody labeled both the CIS and the nuclei but not the COS. The yellow bracket indicates degenerated COS. Double-labeling of cARR and PNA illustrated the following features regarding the relative position of COS and CIS: 1) the COS is narrower than the CIS and the base of the OS is at the transition point (red arrows) and 2) the CIS is the portion above the ONL (the cone nucleus is generally located on the top rows of ONL as indicated by white arrows) and below the OS. Cones were labeled by rhodamine-PNA (in red), and the nuclei were stained with DAPI (blue) in *A*–*I*. (Scale bar, 10 μm in *A*–*F* and 5 μm in *G*–*I*.)

retina that is consistent with the same threshold of rod-mediated responses in both cone types.

Dark Current in *Opn1sw*$^{-/-}$*Opn1mw*$^{-/-}$ Cones. In WT rods and cones, the circulating dark current (mainly carried by Na^{+}) through the cGMP-gated channel keeps photoreceptors in a depolarizing state (25, 26). Activation of the phototransduction cascade by light results in a reduction of the circulating current, which leads to photoreceptor hyperpolarization. Given that *Opn1sw*$^{-/-}$*Opn1mw*$^{-/-}$ cones lack normal COSs and do not respond to light, we asked whether a dark current was still present. We first measured the resting membrane potential of dark-adapted WT and *Opn1sw*$^{-/-}$*Opn1mw*$^{-/-}$ cones without rod input and found it to be similar in both genotypes at

approximately −35 mV (Fig. 7 *A* and *D*). This indicates the presence of an active conductance in the absence of rod–cone coupling and of an outer segment in *Opn1sw*$^{-/-}$*Opn1mw*$^{-/-}$ cones. Next, we tested whether this conductance reflected the presence of the dark current. Because Na^+ is the major carrier of the dark current, reducing extracellular Na^+ would be expected to decrease the current, hyperpolarize the cones, and decrease the amplitude of their photovoltage. Indeed, replacement of Na^+ by choline in WT cones produced a hyperpolarization from −34.20 to −48.20 mV ($n = 5$, $P < 0.01$) (Fig. 7*A*). In addition, we observed a reduction in the cone photoresponse amplitude during Na^+ replacement by up to 80% at the brightest intensities (Fig. 7 *B* and *C*). This effect was reversible as the resting membrane potential returned to about −35 mV after washing out the cells in normal Ringer solution.

In *Opn1sw*$^{-/-}$*Opn1mw*$^{-/-}$ cones, replacement of Na^+ by choline produced a hyperpolarization from −34.35 to −46.86 mV ($P < 0.01$) (Fig. 7*D*), which was similar to the amplitude change observed in WT cones (Fig. 7*A*). As expected, *Opn1sw*$^{-/-}$ *Opn1mw*$^{-/-}$ cones remained insensitive to light before, during, and after Na^+ replacement (Fig. 7 *E* and *F*). The most parsimonious explanation is that the current in *Opn1sw*$^{-/-}$*Opn1mw*$^{-/-}$ cones is carried by residual cGMP-gated channels (Fig. 3*D*) that are insensitive to light because key elements of the phototransduction cascade (e.g., cone opsins and G_αt2) are missing (*Discussion*).

We tested a specific blocker of cGMP-gated channels, L-cis-diltiazem (20 to 150 μM), on the resting and light-evoked changes in membrane potential of rods and cones. Although we observed the expected effects of the drug on the membrane potential of rods (i.e., hyperpolarization of the membrane and decrease in the light-evoked response amplitude), we were not able to detect a clear effect of the drug on the cone membrane potential, either in the WT or in the mutant mice (*SI Appendix*, Table S1). We attribute the failure of this experiment to the fact that the drug, which is water-soluble and was dissolved in the recording pipette, had to diffuse from the site of the clamp (pedicle) all the way up to the CIS that is about 50 μm away. Nonetheless, despite the technical limitations, we recorded a small but significant decrease in resting membrane potential (about −5 mV) in all three recorded *Opn1sw*$^{-/-}$*Opn1mw*$^{-/-}$ cones (*SI Appendix*, Table S1). This result is consistent with the presence of active cGMP channels in these cells.

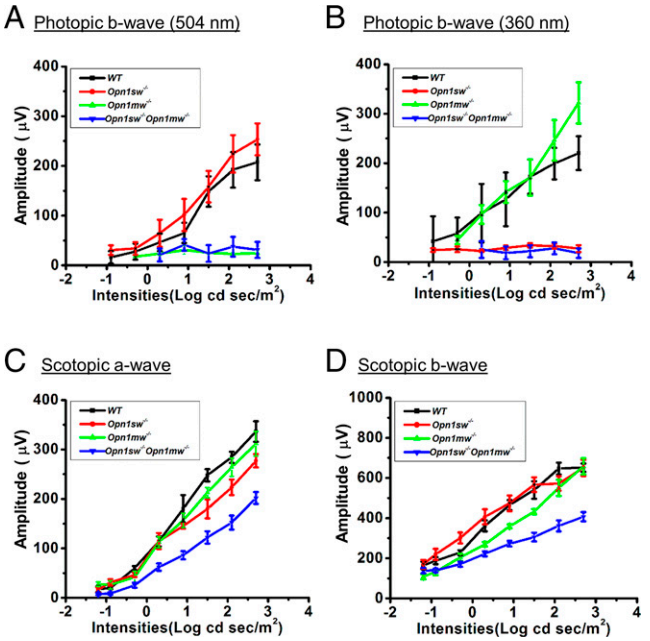

Fig. 4. Photopic and scotopic ERG responses from 1-mo-old *Opn1sw*$^{-/-}$, *Opn1mw*$^{-/-}$, *Opn1sw*$^{-/-}$*Opn1mw*$^{-/-}$, and WT mice. The amplitudes of photopic b-wave responses to (*A*) 504 nm and (*B*) 360 nm stimuli at different light intensities (−0.9, −0.3, 0.3, 0.9, 1.5, 2.1, and 2.7 Log cd s/m^2). The scotopic (*C*) a-wave and (*D*) b-wave amplitudes at different light intensities (−1.2, −0.9, −0.3, 0.3, 0.9, 1.5, 2.1, and 2.7 Log cd s/m^2) to 504 nm light. Data represent mean ± SEM. n = 4, 5, 6, and 8 for WT, *Opn1sw*$^{-/-}$, *Opn1mw*$^{-/-}$, and *Opn1sw*$^{-/-}$*Opn1mw*$^{-/-}$ mice, respectively.

Discussion

By taking a loss-of-function approach, here we show that cone opsins are important for cone disk morphogenesis and outer segment formation. However, the most surprising finding of this work is that cones can survive for an extended time (at least 12 mo) without cone opsins. This finding revises the established dogma based on the absolute requirement of rhodopsin for rod viability. It represents the starkest difference between rod and cone photoreceptors. The reason why cones but not rods can survive without their respective opsins is not clear yet, but we present several possibilities below.

One possibility is the different volume of outer segments between mouse rods and cones. For example, the volume of a mouse COS is ∼1/3 of ROS (36 μm^3 in rods versus 14 μm^3 in cones) (25, 27). Thus, *Opn1sw*$^{-/-}$*Opn1mw*$^{-/-}$ cones only need to degrade ∼1/3 of the proteins destined for the outer segment compared to *Rho*$^{-/-}$ rods. Assuming the protein densities are the same and similar gene regulation mechanisms, this translates into a great reduction in metabolic stress. For primate photoreceptors, this difference is much smaller (40 μm^3 in rods versus 30 μm^3 in cones) (28, 29). This would indicate that primate cones may be more susceptible to cone opsin loss than their murine counterparts. This is indeed the case as cones in human X-linked blue cone monochromacy patients carrying deletions in the red/green opsin gene array can survive in reduced numbers with abnormally shortened outer segments (30). Nevertheless, these patients possess a sufficient number of red/green cones that may warrant future gene augmentation therapy. Thus, the susceptibility of primate cones to cone opsin loss seems to lie between mouse cones and rods and could be related to their relative size. If this hypothesis holds true, we can predict that amphibian rods and cones will exhibit the biggest difference in terms of susceptibility to opsin loss (2,000 μm^3 in rods versus 70 μm^3 in cones) (29, 31). Photoreceptors are the only neurons of central nervous system (CNS) that possess a highly specialized structure of outer segment, which is dedicated to light detection. Our results indicate that an intact outer segment is not essential for cone survival; the degeneration of rods without an outer segment may be caused by a secondary effect (e.g., metabolic stress caused by degradation of large amounts of phototransduction proteins).

Another possibility is that cones are less vulnerable to outer segment disruption compared with rods. Goldfish COSs become shortened and even disappear when living in lower temperature, but they regenerate within approximately a week at room temperature (32). Similarly, the outer segments of ground squirrel cones are much shortened during hibernation, when body temperature can be as low as 4 °C, yet they regrow rapidly after hibernation (33, 34). These data point out the potential to regenerate the COS of patients with red/green opsin deficiency by gene therapy.

Alternatively, cones without opsins may survive because rods can provide them with trophic support. Several viability factors have been identified, including the well-characterized rod-derived cone viability factor (RdCVF), a thioredoxin-like protein secreted by rods that promotes cone survival by increasing glucose intake

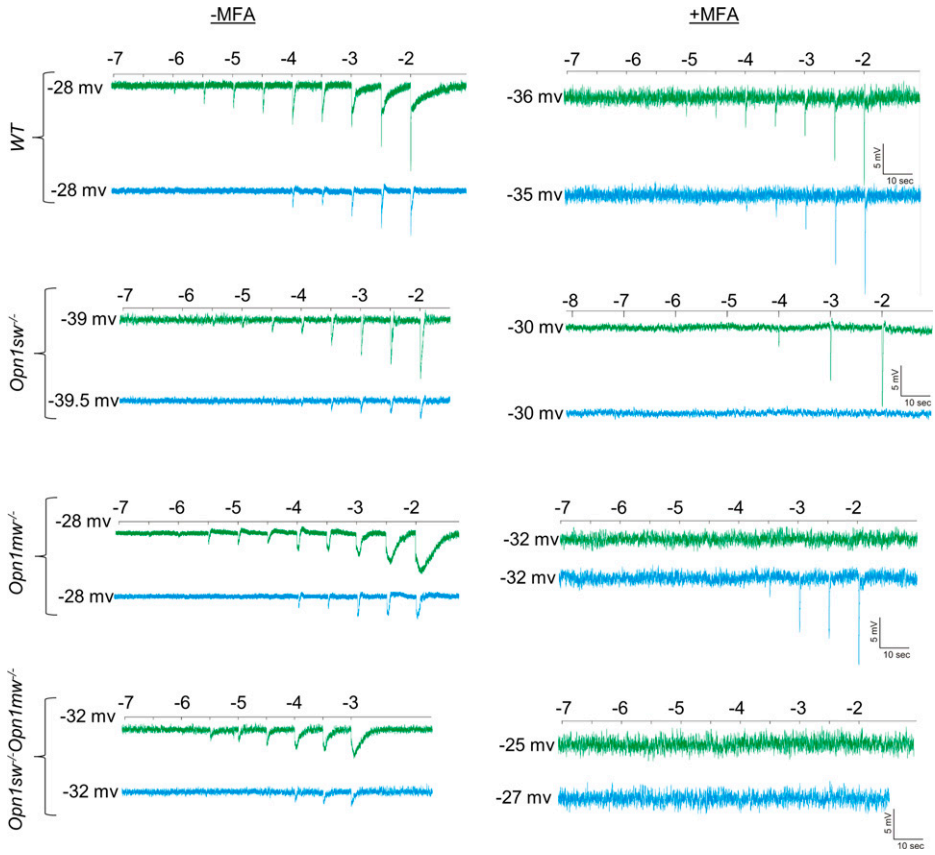

Fig. 5. Cone light responses from *Opn1sw*$^{-/-}$, *Opn1mw*$^{-/-}$, *Opn1sw*$^{-/-}$*Opn1mw*$^{-/-}$, and WT mice. Representative patch-clamp recordings from cone pedicles of 6-mo-old mice of different genotypes in response to 500 nm (green, top trace) or 350 nm (blue, bottom trace) light in the (*Left*) absence or (*Right*) presence of MFA. The numbers in front of each trace indicate the resting membrane potential. The numbers on the top of each panel indicate the logarithmic scale attenuation of 20-ms flash intensity. The unattenuated light intensity is 200,000 photons per μm^2 per flash at 500 nm and 2,000 photons per μm^2 per flash at 350 nm.

in cones and stimulating aerobic glycolysis (35). Because rods outnumber cones by about 30 to 1 (27), rods may provide both metabolic and structural support to the cones (36). In addition, rods and cones may interact metabolically and/or electrically through rod–cone gap junctions, although the exact nature and/or benefit of these interactions remains uncertain. On one hand, rod–cone gap junctions have been proposed to support the diffusion of apoptotic signals from the dying rods to the cones. In degenerative diseases that primarily affect rods such as retinitis pigmentosa, the diffusion of these apoptotic signals may cause the secondary death of overwise healthy cones—a form of "bystander killing" effect (37). Although it has been demonstrated that gap junctions mediate bystander cell death in the retina (38), eliminating Cx36 in the retinal degeneration-1 (rd1) mouse model did not slow down secondary cone loss (39), indicating that the rod–cone coupling role in the secondary death of cones may not be significant or required. On the other hand, rod–cone gap junctions may play a role in supporting cone survival when cones are functionally impaired. Clearly, Cx36 does not appear required for the normal development, function, and maintenance of cones (or of rods), as

Table 1. The threshold intensity of cones and rods from WT, *Opn1sw*$^{-/-}$, *Opn1mw*$^{-/-}$, and *Opn1sw*$^{-/-}$*Opn1mw*$^{-/-}$ mice

	Wavelength (nm)	Cone (+ rod input) (photons/μm^2/20 ms)	Cone (− rod input) (photons/μm^2/20 ms)	Rod (photons/μm^2/20 ms)
WT	500	0.64 ± 0.35 (n = 5)	12.1 ± 3.62 (n = 6)	0.21 ± 0.07 (n = 7)
	350	0.49 ± 0.34 (n = 4)	5.33 ± 2.10 (n = 6)	0.21 ± 0.10 (n = 4)
Opn1sw$^{-/-}$	500	1.17 ± 0.49 (n = 4)	15.8 ± 9.28 (n = 6)	0.07 ± 0.03 (n = 5)
	350	0.15 ± 0.00 (n = 4)	16.7 ± 9.33 (n = 6) ≥ 50 (n = 2)*	1.08 ± 0.98 (n = 5)
Opn1mw$^{-/-}$	500	2.04 ± 1.08 (n = 5)	806 ± 487 (n = 5) ≥ 2,000 (n = 2)†	0.23 ± 0.07 (n = 11)
	350	0.22 ± 0.07 (n = 5)	11.4 ± 9.68 (n = 5)	0.08 ± 0.02 (n = 11)
Opn1sw$^{-/-}$	500	0.74 ± 0.28 (n = 10)	> 2,000 (n = 5)	0.11 ± 0.04 (n = 5)
Opn1mw$^{-/-}$	350	1.03 ± 0.51 (n = 9)	> 50 (n = 5)	0.49 ± 0.26 (n = 5)

Values are mean ± SEM, with the number of cells studied indicated in parentheses. Threshold is the intensity at which the response is ≥ 0.5 mV.
*Two *Opn1sw*$^{-/-}$ cones did not respond to 350 nm light without rod input.
†Two *Opn1mw*$^{-/-}$ cones did not respond to 500 nm light without rod input.

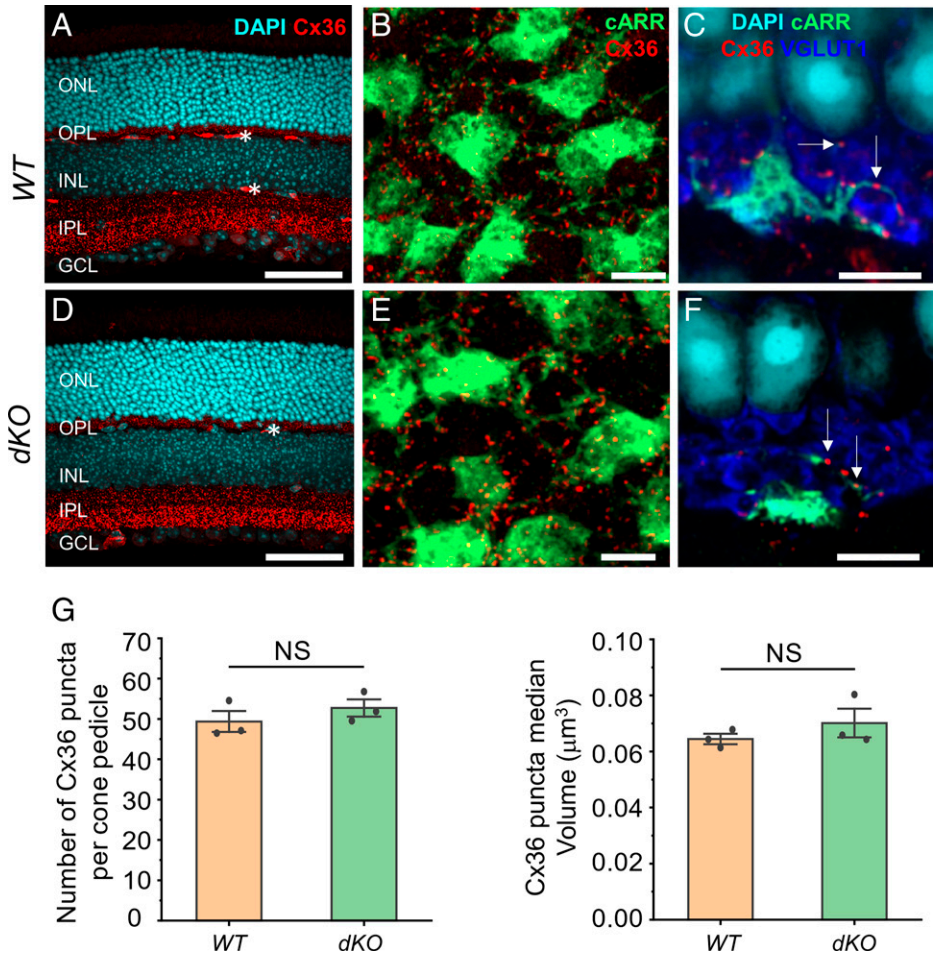

Fig. 6. Cx36 distribution in (*A–C*) WT and (*D–E*) *Opn1sw*$^{-/-}$*Opn1mw*$^{-/-}$ (*dKO*) retinas. (*A* and *D*) Cx36 (red) was expressed in the OPL and IPL in both genotypes on retinal sections. Note the OPL labeling was weaker compared to IPL. Nonspecific labeling of some blood vessels by Cy3 anti-mouse secondary antibody is indicated by white asterisks. (*B* and *E*) Cx36 immuno-puncta (red) were associated with cone telodendria in OPL on whole-mount retinas in both genotypes (green). (*C* and *F*) Representative images showing Cx36 puncta (red) at points of contact (white arrows) between rod spherules (blue) and cone telodendria (green). (*G*) Quantification of the number of Cx36 puncta per cone pedicle and of the median volume of Cx36 puncta at photoreceptor terminals. Data represent mean ± SEM. $n = 3$ mice per genotype. For each animal, a volume of 32 to 41 cone pedicles including between 1,745 and 1,987 Cx36 puncta was surveyed. The mean value of the number of Cx36 puncta per cone pedicle and the median volume of Cx36 puncta were calculated for each animal to generate a single value. NS, $P > 0.05$. Statistical analysis was performed by unpaired two-sample *t* test. Mice were about 2 mo old. Cones were labeled for cone arrestin (cARR; green), rod spherules were labeled for the vesicular glutamate transporter 1 (VGLUT1; blue), and nuclei were stained with DAPI (cyan). INL, inner nuclear layer; GCL, ganglion cell layer. (Scale bar, 50 μm in *A* and *D* and 5 μm in *B*, *C*, *E*, and *F*.)

demonstrated in *Cx36*$^{-/-}$ animals (21, 40). However, a "bystander trophic" effect has been proposed in an experimental mouse model in which loss of Cx36 resulted in increased vulnerability to secondary photoreceptor cell loss following focal laser-induced lesions (41). Thus, Cx36 may contribute to the survival of photoreceptor cells after trauma. Although the nature of the trophic agent exchanged via gap junction coupling remains unknown, it is possible that *Opn1sw*$^{-/-}$*Opn1mw*$^{-/-}$ cones survive because of electrical coupling between rods and cones. In support of this, mutations that either constitutively activate or constitutively inactivate the phototransduction cascade—and therefore keep the membrane constantly hyperpolarized or constantly depolarized—invariably lead to photoreceptor cell death (42). The intriguing possibility that rods may support *Opn1sw*$^{-/-}$*Opn1mw*$^{-/-}$ cone survival by providing the cone membrane with light-evoked signals and thereby offering cones a residual function is supported by our findings. This possibility warrants further investigation.

Although *Opn1sw*$^{-/-}$*Opn1mw*$^{-/-}$ cones survive for an extended time, we found evidence that cones without outer segments affect rod viability and function as reflected by a reduction of ONL length and scotopic ERG a- and b-wave amplitudes of *Opn1sw*$^{-/-}$*Opn1mw*$^{-/-}$ mice compared with WT mice (Fig. 4*C* and *SI Appendix*, Fig. S5). Why does a 3.3% reduction in ONL thickness lead to twofold to threefold reductions in scotopic a-wave of *Opn1sw*$^{-/-}$*Opn1mw*$^{-/-}$ mice? One possibility is that an accumulation of extracellular debris in the subretinal space of *Opn1sw*$^{-/-}$*Opn1mw*$^{-/-}$ mice might affect chromophore supply from RPE to rods.

Previously, *Opn1sw*$^{-/-}$ mouse was shown to respond to 360-nm light albeit with substantially reduced sensitivity by ERG (8). However, we did not observe photopic ERG responses to 360-nm light of *Opn1sw*$^{-/-}$ mouse even at high light intensities (Fig. 4*B*). Mouse M-opsin in individual cones is about 10-fold less sensitive to light at 360 nm than it is at 510 nm (8). In the Ganzfeld ERG, WT mouse absolute b-wave sensitivity at 510 nm (due to M-opsin) is about 0.2× that at 360 nm (due to S-opsin) (43). The net result is that measured with the ERG b-wave, in absolute units, the M-opsin in the WT mouse is at least 50-fold less sensitive to 360-nm light than S-opsin. There are two factors that may contribute to the absence of response

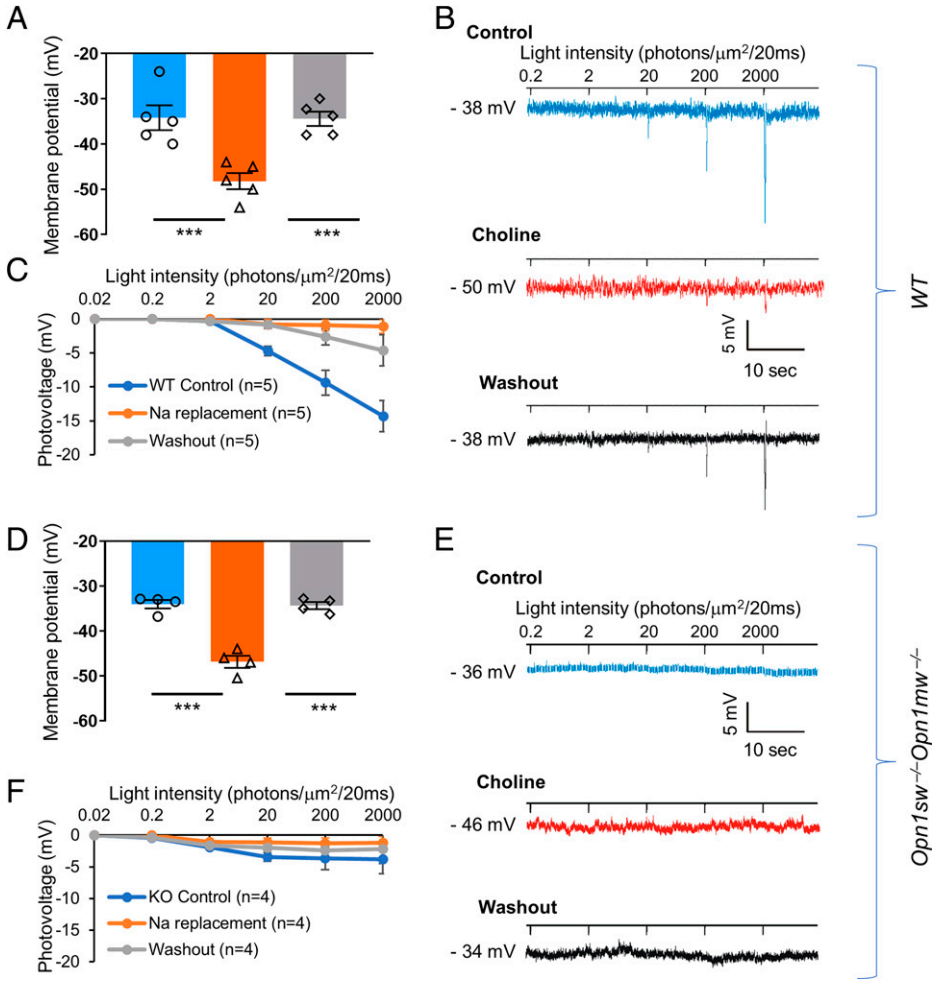

Fig. 7. Effects of Na^+ substitution by choline on photovoltage and resting membrane potential of WT and *Opn1sw*$^{-/-}$*Opn1mw*$^{-/-}$ cones. Resting membrane potential of (*A*) WT and (*D*) *Opn1sw*$^{-/-}$*Opn1mw*$^{-/-}$ cones before, during, and after (i.e., washout) Na^+ replacement. $n = 5$ (WT) and 4 (*Opn1sw*$^{-/-}$ *Opn1mw*$^{-/-}$) cones (one to two cells per animal). Representative recordings of the cone light responses to 20-ms light flashes of increasing intensities (0.2, 2, 20, 200, and 2,000 R*) for (*B*) WT and (*E*) *Opn1sw*$^{-/-}$*Opn1mw*$^{-/-}$ cones. Averaged photovoltage amplitudes from (*C*) five WT and (*F*) four *Opn1sw*$^{-/-}$*Opn1mw*$^{-/-}$ cones (one to two cells per animal) at different intensities before, during, and after Na^+ replacement. Data represent mean ± SEM in *A*, *C*, *D*, and *F*. ***$P < 0.001$ by one-way analysis of variance (ANOVA) with Tukey post hoc analysis in *A* and *D*.

in our experiments: 1) M-opsin is primarily expressed in the dorsal retina (44–46), so that depending on how homogeneously the retina is stimulated, we could be delivering less 360 nm light to the dorsal retina. 2) Because we did our ERG experiments from low intensities to high intensities, the *Opn1sw*$^{-/-}$ mouse might have lost some overall responsivity as the experiment progressed at higher intensities.

Our data clearly show that although *Opn1sw*$^{-/-}$*Opn1mw*$^{-/-}$ cones do not respond to light directly, their membrane potential still senses rod-originated changes in membrane voltage via gap junction. Thus, we have generated an interesting mouse line that separates the two functions mediated by cones, the intrinsic cone photoresponses and transmission of extrinsic rod signals. In this respect, the structure and function of *Opn1sw*$^{-/-}$ *Opn1mw*$^{-/-}$ cones are more like typical CNS neurons in the absence of outer segment and phototransduction. The electrical coupling may help maintain the connectivity of *Opn1sw*$^{-/-}$ *Opn1mw*$^{-/-}$ cones with rods and secondary order neurons (e.g., bipolar cells) and contribute to cone survival because neurons receiving no synaptic stimulation degenerate (47). Another surprising finding is the presence of normal dark current in *Opn1sw*$^{-/-}$ *Opn1mw*$^{-/-}$ cones. The Na^+ replacement experiment suggests that the dark current is mainly carried by Na^+ as in WT cones, although it is not regulated by light. The residual cone cGMP-gated channels are likely responsible for the observed dark current. Since the amount of cone CNGA3 subunits was substantially reduced in *Opn1sw*$^{-/-}$*Opn1mw*$^{-/-}$ cones (Fig. 3*D*), how can they mediate a normal dark current? This might occur because under normal conditions, in the WT, only about 5% or less of the channels are activated in the dark to maintain the dark current (48), suggesting that very few channels are needed to maintain a normal dark current. Thus, our data support the view that residual expression of CNGA3 channels in *Opn1sw*$^{-/-}$ *Opn1mw*$^{-/-}$ cones likely supports a dark current that allows the cells to maintain a quasi-normal resting membrane potential, and this current is not sensitive to changes in light. Since we were unable to detect GC1 in *Opn1sw*$^{-/-}$ *Opn1mw*$^{-/-}$ cones by immunostaining (Fig. 3*A*), it raised the question of the origin of cGMP in *Opn1sw*$^{-/-}$*Opn1mw*$^{-/-}$ cones. An intriguing possibility is that cGMP may flow into *Opn1sw*$^{-/-}$*Opn1mw*$^{-/-}$ cones, which are heavily coupled to neighboring rods via gap junctions (Fig. 6) (21). Gap junctions are permeable to molecules up to 1 kDa in molecular size (49), and cGMP has a molecular size of 345.21 Da. Although the lack of effect of the gap junction blocker MFA on the resting membrane potential of *Opn1sw*$^{-/-}$*Opn1mw*$^{-/-}$ cones would suggest that rods are not the source of cGMP for the mutant cones,

definitive demonstration will require genetic elimination of rod–cone coupling as well as the determination of the turnover of cGMP and other important biological complexities in the electrically isolated mutant cones. Future research will answer the fundamental question of the origin of cGMP.

Finally, although the results with L-diltiazem point toward the involvement of cGMP-gated channels in maintaining depolarized dKO cones, we cannot exclude the contribution of ionic exchangers to the dark current. Indeed, several Na^+/Ca^{2+} and K^+ exchangers (e.g., NCKX2 and NCKX4) have been found in the cones (50, 51). Their relative contribution will require further investigation.

Materials and Methods

Opn1mw$^{-/-}$ and *Opn1sw*$^{-/-}$ mice were generated and genotyped as described previously (8, 9). *Opn1sw*$^{-/-}$ mice were bred with *Opn1mw*$^{-/-}$ mice to obtain *Opn1sw*$^{-/-}$*Opn1mw*$^{-/-}$ mice. Mice were reared under cyclic light (12 h light/12 h dark). Samples were collected during light cycle unless otherwise noted. All animal experiments were approved by the Institutional Animal Care and Use Committees at the University of Utah, The University of Texas Health Science Center in Houston, and the Baylor College of Medicine. All the experiments were performed in accordance with the Association for Research in Vision and Ophthalmology Statement for the Use of Animals in Ophthalmic and Vision Research. Immunodetection and confocal microscopy, ERG, electrophysiological recordings, and transmission electron microscopy were done as previously described (21, 23, 24, 52–55). Detailed methods are described in *SI Appendix, Materials and Methods*.

Data Availability. There is no shared data (e.g., code analyses, sequences, dataset, structural data, genomic and proteomic data, etc.) in this study. All study data are included in the article and/or *SI Appendix*.

ACKNOWLEDGMENTS. We thank Dr. Wing Y. "Joyce" Keung for performing Cx36 staining, Dr. Edward N. Pugh Jr. for providing the *Opn1sw*$^{-/-}$ mice, Dr. Jeannie Chen for providing the S-opsin antibody, and Dr. Xi-Qin Ding for providing cone CNGA3 and CNGB3 antibodies. We also thank Dr. Edward N. Pugh Jr. for help with the revision of the manuscript. This work was supported by NIH grants EY022614 (Y.F.), EY029408 (C.P.R.), and EY029428 (C.-H.S.); Retinal Research Foundation (Y.F.); the Sarah Campbell Blaffer Endowment in Ophthalmology (Y.F.); the Bernice Weingarten Endowment in Ophthalmology (C.P.R.); Stein Innovation Award from Research to Prevent Blindness (C.-H.S.); NIH core grant 2P30EY002520 to Baylor College of Medicine; and an unrestricted grant to the Department of Ophthalmology at Baylor College of Medicine from Research to Prevent Blindness.

1. P. A. Hargrave, J. H. McDowell, Rhodopsin and phototransduction: A model system for G protein-linked receptors. *FASEB J.* **6**, 2323–2331 (1992).
2. J. Nathans, S. L. Merbs, C. H. Sung, C. J. Weitz, Y. Wang, Molecular genetics of human visual pigments. *Annu. Rev. Genet.* **26**, 403–424 (1992).
3. J. Nathans, Rhodopsin: Structure, function, and genetics. *Biochemistry* **31**, 4923–4931 (1992).
4. J. Nathans, D. Thomas, D. S. Hogness, Molecular genetics of human color vision: The genes encoding blue, green, and red pigments. *Science* **232**, 193–202 (1986).
5. A. K. Gross *et al.*, Defective development of photoreceptor membranes in a mouse model of recessive retinal degeneration. *Vision Res.* **46**, 4510–4518 (2006).
6. M. M. Humphries *et al.*, Retinopathy induced in mice by targeted disruption of the rhodopsin gene. *Nat. Genet.* **15**, 216–219 (1997).
7. J. Lem *et al.*, Morphological, physiological, and biochemical changes in rhodopsin knockout mice. *Proc. Natl. Acad. Sci. U.S.A.* **96**, 736–741 (1999).
8. L. L. Daniele *et al.*, A mouse M-opsin monochromat: Retinal cone photoreceptors have increased M-opsin expression when S-opsin is knocked out. *Vision Res.* **51**, 447–458 (2011).
9. H. Xu, N. Enemchukwu, X. Zhong, O. Zhang, Y. Fu, Deletion of M-opsin prevents M cone degeneration in a mouse model of Leber congenital amaurosis. *Am. J. Pathol.* **190**, 1059–1067 (2020).
10. S. M. Conley, M. R. Al-Ubaidi, Z. Han, M. I. Naash, Rim formation is not a prerequisite for distribution of cone photoreceptor outer segment proteins. *FASEB J.* **28**, 3468–3479 (2014).
11. K. Arikawa, L. L. Molday, R. S. Molday, D. S. Williams, Localization of peripherin/rds in the disk membranes of cone and rod photoreceptors: Relationship to disk membrane morphogenesis and retinal degeneration. *J. Cell Biol.* **116**, 659–667 (1992).
12. B. J. Carr, P. Stanar, O. L. Moritz, Distinct roles for prominin-1 and photoreceptor cadherin in outer segment disc morphogenesis in CRISPR-altered *X. laevis*. *J. Cell Sci.* **134**, jcs253906 (2021).
13. D. Chakraborty, S. M. Conley, M. R. Al-Ubaidi, M. I. Naash, Initiation of rod outer segment disc formation requires RDS. *PLoS One* **9**, e98939 (2014).
14. J. Jászai, C. A. Fargeas, M. Florek, W. B. Huttner, D. Corbeil, Focus on molecules: Prominin-1 (CD133). *Exp. Eye Res.* **85**, 585–586 (2007).
15. W. Otsu, Y.-C. Hsu, J.-Z. Chuang, C.-H. Sung, The late endosomal pathway regulates the ciliary targeting of tetraspanin protein peripherin 2. *J. Neurosci.* **39**, 3376–3393 (2019).
16. Z. Yang *et al.*, Mutant prominin 1 found in patients with macular degeneration disrupts photoreceptor disk morphogenesis in mice. *J. Clin. Invest.* **118**, 2908–2916 (2008).
17. S. Zacchigna *et al.*, Loss of the cholesterol-binding protein prominin-1/CD133 causes disk dysmorphogenesis and photoreceptor degeneration. *J. Neurosci.* **29**, 2297–2308 (2009).
18. M. A. El-Brolosy, D. Y. R. Stainier, Genetic compensation: A phenomenon in search of mechanisms. *PLoS Genet.* **13**, e1006780 (2017).
19. S. Asteriti, C. Gargini, L. Cangiano, Mouse rods signal through gap junctions with cones. *eLife* **3**, e01386 (2014).
20. E. P. Hornstein, J. Verweij, P. H. Li, J. L. Schnapf, Gap-junctional coupling and absolute sensitivity of photoreceptors in macaque retina. *J. Neurosci.* **25**, 11201–11209 (2005).
21. N. Jin *et al.*, Molecular and functional architecture of the mouse photoreceptor network. *Sci. Adv.* **6**, eaba7232 (2020).
22. C. Ribelayga, Y. Cao, S. C. Mangel, The circadian clock in the retina controls rod-cone coupling. *Neuron* **59**, 790–801 (2008).
23. N. G. Jin, A. Z. Chuang, P. J. Masson, C. P. Ribelayga, Rod electrical coupling is controlled by a circadian clock and dopamine in mouse retina. *J. Physiol.* **593**, 1597–1631 (2015).
24. F. Pan, S. L. Mills, S. C. Massey, Screening of gap junction antagonists on dye coupling in the rabbit retina. *Vis. Neurosci.* **24**, 609–618 (2007).
25. Y. Fu, K. W. Yau, Phototransduction in mouse rods and cones. *Pflugers Arch.* **454**, 805–819 (2007).
26. K. W. Yau, Phototransduction mechanism in retinal rods and cones. The Friedenwald Lecture. *Invest. Ophthalmol. Vis. Sci.* **35**, 9–32 (1994).
27. L. D. Carter-Dawson, M. M. LaVail, Rods and cones in the mouse retina. I. Structural analysis using light and electron microscopy. *J. Comp. Neurol.* **188**, 245–262 (1979).
28. D. A. Baylor, B. J. Nunn, J. L. Schnapf, The photocurrent, noise and spectral sensitivity of rods of the monkey *Macaca fascicularis*. *J. Physiol.* **357**, 575–607 (1984).
29. E. N. Pugh Jr., T. D. Lamb, "Phototransduction in vertebrate rods and cones: Molecular mechanisms of amplification, recovery and light adaptation" in *Handbook of Biological Physics, Molecular Mechanisms of Visual Transduction*, D. G. Stavenga, W. J. de Grip, E. N. Pugh Jr., Eds. (Elsevier Science B.V., 2000), pp. 183–255.
30. A. V. Cideciyan *et al.*, Human cone visual pigment deletions spare sufficient photoreceptors to warrant gene therapy. *Hum. Gene Ther.* **24**, 993–1006 (2013).
31. D. A. Baylor, B. J. Nunn, Electrical properties of the light-sensitive conductance of rods of the salamander *Ambystoma tigrinum*. *J. Physiol.* **371**, 115–145 (1986).
32. W. W. Dawson, G. M. Hope, J. J. Bernstein, Goldfish retina structure and function in extended cold. *Exp. Neurol.* **31**, 368–382 (1971).
33. T. Kuwabara, Cytologic changes of the retina and pigment epithelium during hibernation. *Invest. Ophthalmol.* **14**, 457–467 (1975).
34. C. E. Remé, R. W. Young, The effects of hibernation on cone visual cells in the ground squirrel. *Invest. Ophthalmol. Vis. Sci.* **16**, 815–840 (1977).
35. N. Aït-Ali *et al.*, Rod-derived cone viability factor promotes cone survival by stimulating aerobic glycolysis. *Cell* **161**, 817–832 (2015).
36. C. Punzo, K. Kornacker, C. L. Cepko, Stimulation of the insulin/mTOR pathway delays cone death in a mouse model of retinitis pigmentosa. *Nat. Neurosci.* **12**, 44–52 (2009).
37. H. Ripps, Cell death in retinitis pigmentosa: Gap junctions and the 'bystander' effect. *Exp. Eye Res.* **74**, 327–336 (2002).
38. K. Cusato *et al.*, Gap junctions mediate bystander cell death in developing retina. *J. Neurosci.* **23**, 6413–6422 (2003).
39. K. Kranz, F. Paquet-Durand, R. Weiler, U. Janssen-Bienhold, K. Dedek, Testing for a gap junction-mediated bystander effect in retinitis pigmentosa: Secondary cone death is not altered by deletion of connexin36 from cones. *PLoS One* **8**, e57163 (2013).
40. M. R. Deans, B. Volgyi, D. A. Goodenough, S. A. Bloomfield, D. L. Paul, Connexin36 is essential for transmission of rod-mediated visual signals in the mammalian retina. *Neuron* **36**, 703–712 (2002).
41. K. Striedinger *et al.*, Loss of connexin36 increases retinal cell vulnerability to secondary cell loss. *Eur. J. Neurosci.* **22**, 605–616 (2005).
42. G. L. Fain, J. E. Lisman, Light, Ca^{2+}, and photoreceptor death: New evidence for the equivalent-light hypothesis from arrestin knockout mice. *Invest. Ophthalmol. Vis. Sci.* **40**, 2770–2772 (1999).
43. A. L. Lyubarsky, B. Falsini, M. E. Pennesi, P. Valentini, E. N. Pugh Jr., UV- and midwave-sensitive cone-driven retinal responses of the mouse: A possible phenotype for coexpression of cone photopigments. *J. Neurosci.* **19**, 442–455 (1999).
44. M. L. Applebury *et al.*, The murine cone photoreceptor: A single cone type expresses both S and M opsins with retinal spatial patterning. *Neuron* **27**, 513–523 (2000).
45. K. C. Eldred, C. Avelis, R. J. Johnston Jr., E. Roberts, Modeling binary and graded cone cell fate patterning in the mouse retina. *PLOS Comput. Biol.* **16**, e1007691 (2020).
46. S. S. Nikonov, R. Kholodenko, J. Lem, E. N. Pugh Jr., Physiological features of the S- and M-cone photoreceptors of wild-type mice from single-cell recordings. *J. Gen. Physiol.* **127**, 359–374 (2006).

47. N. L. Mata *et al.*, Delayed dark-adaptation and lipofuscin accumulation in abcr$^{+/-}$ mice: Implications for involvement of ABCR in age-related macular degeneration. *Invest. Ophthalmol. Vis. Sci.* **42**, 1685–1690 (2001).
48. P. Bauer, "The complex of cGMP-gated channel and Na/Ca^{2+}, K exchanger in rod photoreceptors" in *Madame Curie Bioscience Database* (Landes Bioscience, Austin, TX, 2000–2013). https://www.ncbi.nlm.nih.gov/books/NBK6380/. Accessed 14 August 2021.
49. A. L. Harris, Emerging issues of connexin channels: Biophysics fills the gap. *Q. Rev. Biophys.* **34**, 325–472 (2001).
50. K. Sakurai, F. Vinberg, T. Wang, J. Chen, V. J. Kefalov, The Na(+)/Ca(2+), K(+) exchanger 2 modulates mammalian cone phototransduction. *Sci. Rep.* **6**, 32521 (2016).
51. F. Vinberg *et al.*, The Na^{+}/Ca^{2+}, K^{+} exchanger NCKX4 is required for efficient cone-mediated vision. *eLife* **6**, e24550 (2017).
52. T. Zhang *et al.*, Genetic deletion of S-opsin prevents rapid cone degeneration in a mouse model of Leber congenital amaurosis. *Hum. Mol. Genet.* **24**, 1755–1763 (2015).
53. T. Zhang, N. Zhang, W. Baehr, Y. Fu, Cone opsin determines the time course of cone photoreceptor degeneration in Leber congenital amaurosis. *Proc. Natl. Acad. Sci. U.S.A.* **108**, 8879–8884 (2011).
54. C. Ribelayga, S. C. Mangel, A circadian clock and light/dark adaptation differentially regulate adenosine in the mammalian retina. *J. Neurosci.* **25**, 215–222 (2005).
55. J.-Z. Chuang, S.-Y. Chou, C.-H. Sung, Chloride intracellular channel 4 is critical for the epithelial morphogenesis of RPE cells and retinal attachment. *Mol. Biol. Cell* **21**, 3017–3028 (2010).